The Flory−Huggins Interaction Parameter in Blends of Polystyrene and Poly(*p*-Methylstyrene) by Small-Angle Neutron Scattering

J. D. Londono* and G. D. Wignall

Oak Ridge National Laboratory, Oak Ridge, Tennessee 37831-6197

Received January 22, 1997; Revised Manuscript Received April 28, 1997[⊗]

ABSTRACT: Blends of polystyrene and poly(*p*-methylstyrene) (PPMS) were studied by small-angle neutron scattering. Doubling the molecular weight of the PPMS component had no effect on the Flory−Huggins interaction parameter, χ, as determined from the scattering measurements. The temperature dependence of χ is presented also.

Introduction

The Flory−Huggins interaction parameter, χ, for blends of polystyrene (PS) and poly(*p*-methylstyrene) (PPMS) was determined earlier by Jung and Fischer,[1] and a preliminary report of the present work has also appeared.[2] In this work, we investigate the effect on χ of doubling the molecular weight of the PPMS component. Only the central range of composition ($0.25 \leq \phi \leq 0.75$) is considered. A strong dependence of $\chi(\phi)$ at the extremes in composition has been determined[3] for other systems, yet these effects are small in the central composition range.[4] The results presented here may aid in the understanding of the relationship between monomer architecture, structural asymmetry of blend components, and polymer miscibility.[5]

Experimental Section

The homopolymers were obtained from Polymer Standards Service, Mainz, Germany. Details are shown in Table 1. The blend components were dissolved in toluene, and these solutions were mixed by volume. Methanol was used to precipitate the blends. The resultant white paste was dried at 170 °C overnight. A hard glassy material, either clear or cloudy depending on composition, was formed on cooling. The molecular weight had to be kept low to avoid demixing within the experimental temperature window. As a result, most of the samples were difficult to contain above the glass transition because of the low viscosity. To overcome this difficulty, the blend material was loaded into Al cups of 15 mm i.d. and 0.5 mm bottom thickness. A 0.5 mm thick disk served as a lid and matched closely the inside diameter of the cup. A PTFE O-ring and a 1 kg weight were placed over the lid, and the whole arrangement was placed in a vacuum oven for 4 h at about 160 °C. Prior to the small-angle neutron scattering (SANS) measurements, the samples were placed in sample containers that allowed the O-ring to be squeezed onto the lid, preventing the loss of sample. SANS measurements were performed on samples about 0.7 mm in thickness contained between 0.5 mm thick Al disks. An example of sample designation is S1M150, where the number 50 refers to the approximate weight percent of the PS component, in this case S1. The blend compositions of the samples prepared are listed in Table 2.

The data were collected at the W. C. Koehler 30m SANS facility[6] at the Oak Ridge National Laboratory (ORNL) via a 64×64 cm^2 area detector with cell (element) size $\sim$1 cm^2 and a neutron wavelength (λ) of 4.75 Å. The sample-to-detector distances (SDDs) used were 14 and 3.7 m. The low Q data collected at long SDD are most sensitive to χ, while the high Q data collected at short SDD are most sensitive to the statistical segment length.[7] The data were corrected for instrumental backgrounds and detector efficiency on a cell-by-cell basis prior to radial averaging, to give a Q-range of $5 \times 10^{-3} < Q = 4\pi\lambda^{-1} \sin\theta < 0.04$ Å^{-1} for SDD = 14 m, and $0.02 < Q < 0.17$ Å^{-1} for SDD = 3.7 m, where 2θ is the angle of scatter. The coherent intensities of the sample were obtained by subtracting the intensities of an empty cell. The scattering from the Al of the cells was larger than that in other materials, quartz for example, and varied between cells, and empty subtraction generally left a residual contribution observable at $Q < 0.01$ Å^{-1}, which varied as Q^{-4}, see below. The net intensities were converted to an absolute (±4%) differential cross section per unit sample volume [$d\Sigma/d\Omega(Q)$, in units of cm^{-1}] by comparison with precalibrated secondary standards, based on the measurement of beam flux, vanadium incoherent cross section, and the scattering from water and other reference materials.[8] The detector efficiency calibration was based on the scattering from light water, and this led to angle-independent scattering for vanadium, H-polymer blanks, and water samples of different thicknesses in the range 1−10 mm.

The temperature and sample position of a four-position furnace were controlled via an IEEE-488 interface from the system's computer. The temperature stability of the furnace and the accuracy of temperature measurement were within ±2 °C. Typically, SANS data were collected on a sample at several temperatures in the range 140−220 °C, and the thickness and transmission were recorded at the initial and final temperatures. The sample transmission was measured as described previously.[9] The cross sections of unlabeled (PPMS-H) and fully labeled (PS-D) blanks were also measured as a basis for subtracting the coherent and incoherent backgrounds. These backgrounds were subtracted via empirical methods from the blend intensities.[10]

The intensity scale was calibrated in absolute units at 14 and 3.7 m independently. The overlap between data sets

Table 1. Sample Details

polymer	sample	M_w	N	M_w/M_n
PS-d_8 (deuterated polystyrene)	S1	32 700	291	1.05
	J+F[a]	35 100	338	
PPMS [poly(*p*-methylstyrene)]	M1	58 800	498	1.04
	M2	131 000	1108	1.05
	J+F	63 500	537	

[a] Jung and Fischer.[1]

Table 2. Blend Details: $\chi \times 10^3 = a + (b \times 10^3)/T$ (K)

sample	a	b (K)	demixing temperature (°C)	ϕ_{PSD}
S1M125	-11 ± 1	7.0 ± 0.5		0.2500
S1M150	-8.1 ± 0.9	5.7 ± 0.4	150	0.4996
S1M175	-8.3 ± 0.9	6.1 ± 0.4	150	0.7485
S1M225	-11.9 ± 0.6	7.2 ± 0.3	140	0.2490
S1M250			190	0.5006
S1M275			>220	0.7451

[⊗] Abstract published in *Advance ACS Abstracts,* June 1, 1997.

S0024-9297(97)00070-3 CCC: $14.00

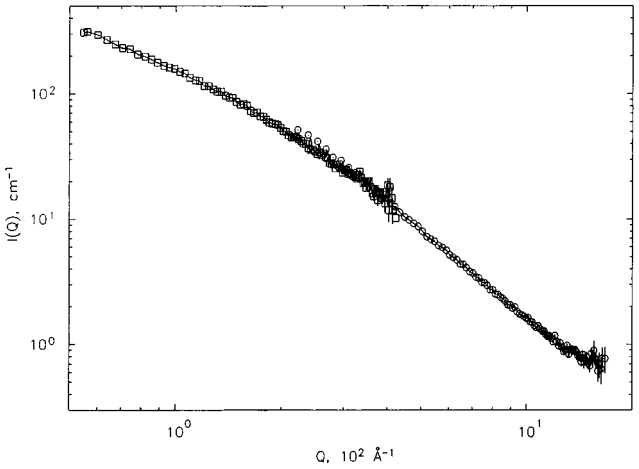

Figure 1. Blend S1M250 at 110 °C. □: Data collected at sample-to-detector distance (SDD) of 14 m. ○: Data collected at SDD of 3.7 m.

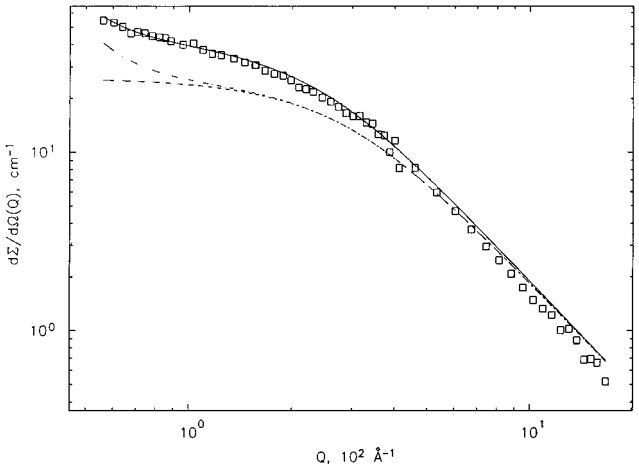

Figure 2. Sample S1M125 at 210 °C. □: Merged data set, from 3.7 and 14m data. —: iRPA fit. - - -: Single-chain contribution (SCC). —•—: SCC with container contribution included. Selected points plotted for clarity.

collected at different SDDs, but the same T and ϕ, was acceptable, and Figure 1 shows a typical pair of data sets. Merged data sets were obtained by binning the 3.7 and 14 m data within the overlap range, while preserving within this range the resolution of the 3.7 m data and overall counting statistics. Figure 2 shows a merged data set. Data at 3.7 m were collected only for a few temperatures. About two-thirds of the data sets consisted only of 14 m data, and one of these data sets is shown in Figure 3.

Data Analysis

The corrected coherent scattering cross section $[d\Sigma/d\Omega(Q)]_{COH}$ is related to the structure factor, $S(Q)$, by

$$\left[\frac{d\Sigma}{d\Omega}(Q)\right]_{COH} = A_0\left(\frac{a_A}{v_A} - \frac{a_B}{v_B}\right)^2 S(Q) \qquad (1)$$

where

$$a_i = \sum_j b_{ij} \qquad (2)$$

and b_{ij} is the scattering length of atom j in the repeat unit of type i. The repeat unit types are denoted by A or B when referring to PS (repeat unit C_8D_8) or PPMS (repeat unit C_9H_{10}), respectively. The ratio of segmental volumes $v_A/v_B = 0.873$,[11] and the reference volume $v_0 = (v_A v_B)^{1/2}$. A_0 is Avogadro's number. The structure factors were fitted via the iRPA[12] expression,

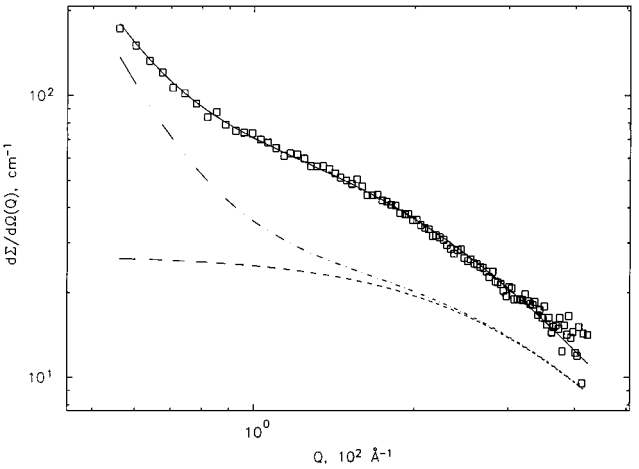

Figure 3. As Figure 2, but for sample S1M125 at 140 °C.

$$\frac{1}{S(Q)} = \frac{1}{N_A\phi_A g_A(x) v_A} + \frac{1}{N_B\phi_B g_B(x) v_B} - \frac{2\chi}{v_0} \qquad (3)$$

The single-chain structure function was assumed to be of the Debye form,

$$g(x) = \frac{2}{x^2}[x - 1 + e^{-x}] \qquad (4)$$

$$x = R_g{}^2 Q^2 \qquad (5)$$

$$R_g{}^2 = Na^2/6 \qquad (6)$$

where R_g and N are the radius of gyration and degree of polymerization of the molecules. The values of the statistical segment lengths of the homopolymers were taken to be $a_A = 0.70$ nm for PS[13,14] and $a_B = 0.76$ nm for PPMS.[14,15]

The subtraction of the contribution from the empty container was never perfect, as the void scattering from the Al was larger than ideal, as discussed above. Thus, the effect of the container was generally observed at $Q < 0.01$ Å^{-1}. This difficulty was overcome by fitting, in addition to χ in eq 3, the prefactor of the Q^{-4} term in the following expression:

$$\left[\frac{d\Sigma}{d\Omega}(Q)\right]_{TOT} = \left[\frac{d\Sigma}{d\Omega}(Q)\right]_{COH} + AQ^{-4} \qquad (7)$$

The additional term is due to Porod scattering from the contrast between Al and the pores of the container material. Figures 2 and 3 show typical fits. Additionally, these figures show $[d\Sigma/d\Omega(Q)]_{COH}(\chi = 0)$, i.e., the contribution from the first two terms in eq 3 (single-chain contribution), with and without the Porod term added. Figures 2 and 3 show that the presence of χ increases the intensity significantly in the range $Q < 0.03$ Å^{-1}, while the Porod term is only significant for $Q < 0.01$ Å^{-1}. Therefore, there is a considerable range in Q for which the contribution due to χ is significantly larger than the single-chain contribution, but for which the container contribution is small. Two strategies were followed in the process of fitting the data. In the first strategy, all the data were included in the fit, and the prefactor in the Porod term was adjusted. In the second

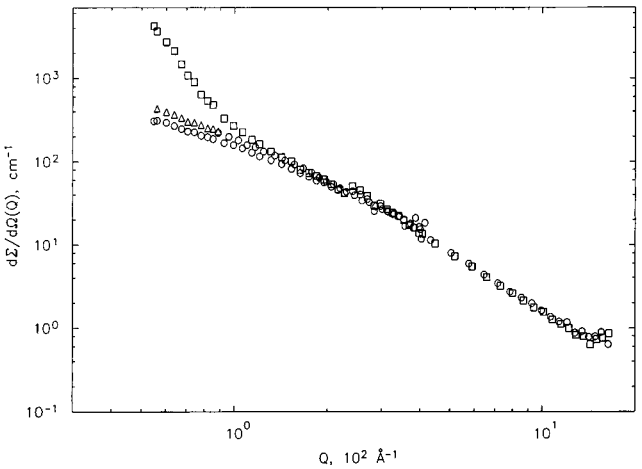

Figure 4. Sample S1M175. □: 150 °C. △: 160 °C. ○: 170 °C. Selected points plotted for clarity.

strategy, only data with $Q > 0.01$ Å^{-1} were included in the fit, and the prefactor of the Porod term was set to null.

Phase separation leads to two well-known effects:[16] the development of a Porod regime (Q^{-4}) at low Q, and the decrease in intensity at high Q (Q^{-2} regime). As Figure 4 demonstrates, the development of the Porod regime in the present set of samples is apparent much earlier, and is vastly more dramatic, than the decrease of the intensity at high Q. As shown in Figure 4, for sample S1M175, the Porod contribution from phase-segregated domains appeared after a drop in temperature of 10 °C, and this contribution was roughly 1 order of magnitude larger than the Porod contribution from the container. In addition, the linear nature of the χ vs T^{-1} dependence disappeared on phase segregation. Therefore, the Q^{-4} term, added to fit the container contribution, does not preclude the distinction between phase-separated and homogeneous mixtures. The small deviations of the model from the data evident in Figure 2 at high Q are of the order of 0.1 cm^{-1} and are likely due to the combination of small systematic errors in intensity calibration, statistical segment length, and volume fraction. It is unlikely that χ is strongly affected by these errors.

Results

The values of χ obtained from the iRPA fits to the data from the homogeneous samples are shown in Figure 5. All samples except S1M125 demixed within the experimental temperature range (140−220 °C), and sample S1M275 was phase-separated within this range. The demixing temperature for each sample is shown in Table 2 to the nearest 10 °C. For some of the samples, data were collected at more than five temperatures within the homogeneous region. The data for these samples were fitted to the expected linear dependence on T^{-1}. Figure 5 shows some of the regression lines that resulted from these fits, and Table 2 shows the regression parameters of all the fits attempted. The values of the regression parameters were independent of the fitting strategy within the quoted error, indicating that the results are independent of the container contribution to the scattering.

Discussion

The molecules in our samples comprised roughly 500−1000 repeat units and, as such, were long enough

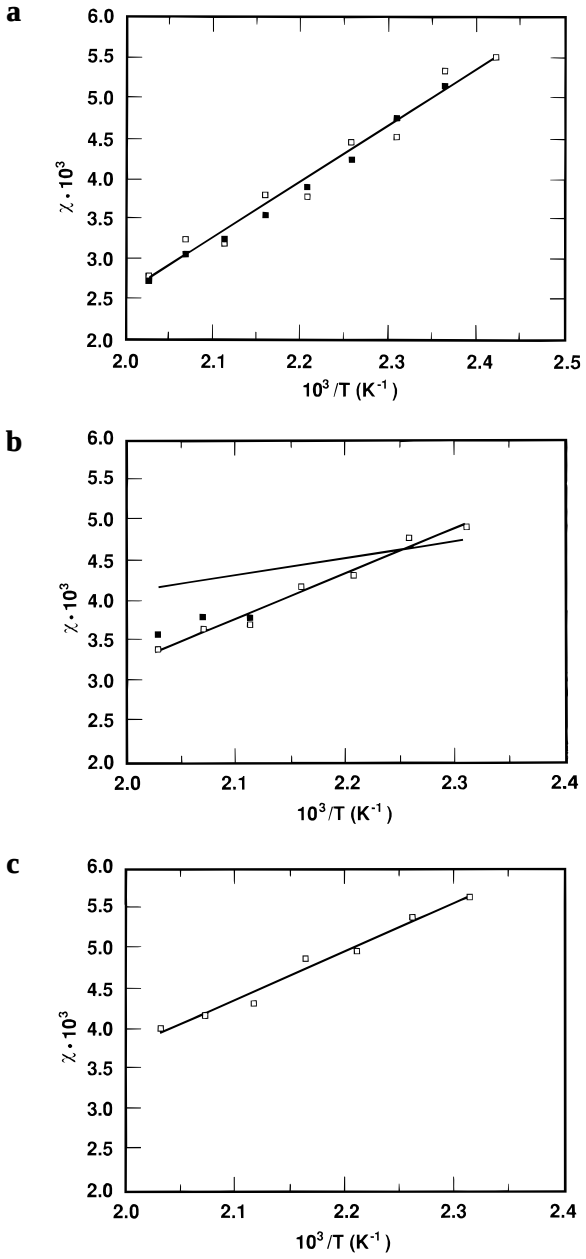

Figure 5. (a) □: χ(T) for blend S1M125, and its regression line. ■: χ(T) for blend S1M225. (b) □: χ(T) for blend S1M150, and its regression line. ■: χ(T) for blend S1M250. The function $\chi(T)$ as determined by Jung and Fischer[1] is shown also. (c) χ(T) for blend S1M175.

to be considered polymeric. Further increase in the chain length of either component led to demixing at higher temperatures, decreasing the dynamic experimental range. In the results presented, demixing already occurred within the experimental window for most samples. Further increase in chain length of the PS component led to a phase-separated blend at all temperatures (S5M150, $M_w = 87\,000$ for homopolymer S5). A decrease in chain length by even a factor of 2 would have led to chains too short to be considered polymeric.

Doubling the molecular weight of the PPMS component did not change the χ parameter. Also, a linear variation of χ with T^{-1} was observed. The agreement of the results for sample S1M150 with those of Jung and Fischer[1] is reasonable (see Figure 5b with molecular parameters in Table 1), considering that the difference in statistical segment length between the blend components was not taken into account in the earlier report.

Acknowledgment. This research was sponsored by The Division of Materials Sciences, U.S. Department of Energy, at the Oak Ridge National Laboratory, managed by Lockheed Martin Energy Research Corp. under Contract DE-AC05-96OR22464. This research was supported in part by an appointment to the Oak Ridge National Laboratory Postdoctoral Research Associates Program, administered jointly by the Oak Ridge National Laboratory and the Oak Ridge Institute for Science and Education.

References and Notes

(1) Jung, W. G.; Fischer, E. W. *Makromol. Chem., Macromol. Symp.* **1988**, *16*, 281.
(2) Xenopoulos, A.; Londono, J. D.; Wignall, G. D.; Wunderlich, B. *Mater. Res. Soc. Symp. Proc.* **1993**, *321*, 107.
(3) Londono, J. D.; Narten, A. H.; Wignall, G. D.; Honnell, K. G.; Hsieh, E. T.; Johnson, T. W.; Bates, F. S. *Macromolecules* **1994**, *27*, 2864. Bates, F. S.; Muthukumar, M.; Wignall, G. D.; Fetters, L. J. *J. Chem. Phys.* **1988**, *89*, 535.
(4) Bidkar, U. R.; Sanchez, I. C. *Macromolecules* **1995**, *28*, 3963. Taylor, J. K.; Debenedetti, P. G.; Graessley, W. *Macromolecules* **1996**, *29*, 764.
(5) Fredrickson, G. H.; Liu, A. J.; Bates, F. S. *Macromolecules* **1994**, *27*, 2503. Pesci, A. I.; Freed, K. F. *J. Chem Phys.* **1989**, *90*, 2003. Curro, J. G. *Macromolecules* **1994**, *27*, 4665. Schweizer, K. S. *Macromolecules* **1993**, *26*, 6050.
(6) Koehler, W. C. *Physica* (*Utrecht*) **1986**, *137B*, 320.
(7) Bates, F. S.; Dierker, S. B.; Wignall, G. D. *Macromolecules* **1986**, *19*, 1938.
(8) Wignall, G. D.; Bates, F. S. *J. Appl. Crystallogr.* **1986**, *20*, 28.
(9) Alamo, R. A.; Londono, J. D.; Mandelkern, L.; Stehling, F. C.; Wignall, G. D. *Macromolecules* **1994**, *27*, 411.
(10) Hayashi, H.; Flory, P. J.; Wignall, G. D. *Macromolecules* **1983**, *16*, 1328.
(11) Patnode, W.; Scheiber, W. J. *J. Am. Chem. Soc.* **1939**, *61*, 3449. Corneliussen, R.; Rice, S. A.; Yamakawa, H. *J. Chem. Phys.* **1963**, *38*, 1768.
(12) de Gennes, P.-G. *Scaling Concepts in Polymer Physics*; Cornell University Press: Ithaca, NY, 1979.
(13) Bates, F. S.; Wignall, G. D. *Phys. Rev. Lett.* **1986**, *57*, 1429. Wignall, G. D.; Hendricks, R. W.; Koehler, W. C.; Lin, J. S.; Wai, M. P.; Thomas, E. L.; Stein, R. S. *Polymer* **1981**, *22*, 886. Fukuda, M.; Fukutomi, M.; Kato, Y.; Hashimoto, T. *J. Polym. Sci., Polym. Phys. Ed.* **1974**, *12*, 871. Miyaki, Y.; Einaga, Y.; Fujita, H. *Macromolecules* **1978**, *11*, 1180.
(14) Maconnachie, A.; Fried, J. R.; Tomlins, P. E. *Macromolecules* **1989**, *22*, 4606.
(15) Tanaka, G.; Imai, S.; Yamakawa, H. *J. Chem. Phys.* **1970**, *52*, 2639.
(16) Londono, J. D.; Wignall, G. D.; Alamo, R. G.; Mandelkern, L.; Stehling, F. C. *Mater. Res. Soc. Symp. Proc.* **1995**, *376*, 281. Alamo, R. G.; Graessley, W. W.; Krishnamoorti, R.; Lohse, D. J.; Londono, J. D.; Mandelkern, L.; Stehling F. C.; Wignall G. D. *Macromolecules* **1997**, *30*, 561.

MA970070Z